PERGAMON

Journal of Quantitative Spectroscopy &
Radiative Transfer 81 (2003) 147–165

Journal of
Quantitative
Spectroscopy &
Radiative
Transfer

www.elsevier.com/locate/jqsrt

Characterization of electron states in dense plasmas and its use in atomic kinetics modeling

D.V. Fisher*,[1], Y. Maron

Faculty of Physics, Weizmann Institute of Science, Rehovot 76100, Israel

Accepted 15 February 2003

Abstract

We describe a self-consistent statistical approach to account for plasma density effects in collisional-radiative kinetics. The approach is based on the characterization of three distinct types of electron states, namely, bound, collectivized, and free, and on the formalism of the effective statistical weights (ESW) of the bound states. The present approach accounts for individual and collective effects of the surrounding electrons and ions on atomic (ionic) electron states. High-accuracy expressions for the ESWs of bound states have been derived. The notions of ionization stage population, free electron density, and rate coefficient are redefined in accordance with the present characterization scheme. The modified expressions for the probabilities of electron-impact induced transitions as well as spontaneous and induced radiative transitions are then obtained. The influence of collectivized states on a dense plasma ionization composition is demonstrated to be strong. Examples of calculated ESWs and populations of ionic quantum states for steady state and transient plasmas are given.

Keywords: Density effects; Collisional-radiative kinetics; Collectivized states; Statistical approach

---

1. Introduction

Remarkable progress has been achieved in recent years in the field of controlled production of dense nonideal plasmas [1,2]. However, an accurate self-consistent modeling of thermodynamics, atomic kinetics, spectra, and transport properties of such plasmas is yet to be achieved. At present, the existing atomic kinetic models and collisional-radiative (CR) codes are based on an oversimplified description of electron states in plasmas. This fact may be responsible, at least partially, for substantial disagreements often found in plasma compositions and spectra calculated using different CR codes.

---

* Corresponding author.
E-mail address: fndima@plasma-gate.weizmann.ac.il (D.V. Fisher).
[1] Present address: Soreq NRC, Yavne 81800, Israel.

0022-4073/03/$ - see front matter © 2003 Elsevier Science Ltd. All rights reserved.
doi:10.1016/S0022-4073(03)00068-2

Majority of the existing models and codes are based on two assumptions. The first assumption is that all the ions of a given ionization stage are immersed in an identical local environment and, consequently, have an identical level scheme. The second assumption is that there exist only two types of electron states in plasma, namely, the unperturbed states bound to a single ion and the free electron states. Usually, for every ionization stage Z the list of unperturbed bound energy levels is truncated at some level by a lowered ionization threshold I_Z, identically for all ions of that Z, and above I_Z only free electron states are considered. (The free-electron continuum is appropriately shifted down in energy, to start at I_Z). In this work, we refer to such an approach to plasma composition modeling as a "traditional approach". The value of I_Z depends on plasma density and composition. Thus, nonphysical discontinuities are introduced into the plasma thermodynamic potentials, arising each time a certain electron state emerges or disappears at once [3] in all the ions of a given element and ionization stage as the plasma density varies.

In reality, both of the above assumptions are substantially oversimplifying the physical picture. First, each ion in plasma is surrounded by a unique spatial arrangement of the perturbing charges. Therefore, disappearance of a certain energy level in an ensemble of ions is gradual, described by the fraction of ions that are perturbed strongly enough by their charged neighbors. Second, the degree of perturbation of an atomic (ionic) electron state by a plasma environment is characterized by continuous parameters, such as the distance to the nearest neighbor ion or the spatial distribution of the local microfield. Therefore, the transformation of an electron state from being bound to a single parent ion and unperturbed to being a part of the positive-energy continuum is gradual rather than abrupt, and proceeds via collectivization of that state among an increasing number of ions in plasma.

One way to remove at least a part of these simplifications (and to resolve the problems they cause) is to turn to a self-consistent average-atom treatment, of which the INFERNO model [4–6] is probably the best-known prototype. The average-atom treatment accounts for the electron state perturbation by density effects (i.e., by collective effects of the plasma environment, but not by an individual effects of the nearest neighbors). However, like the traditional approaches, the average-atom descriptions do not account for variation of local conditions between individual ion locations in plasmas. Thus, they apply primarily to liquid metals and to very strongly coupled plasmas, both classical and Fermi-degenerate, where the near ordering in ion subsystem is well pronounced and all the ions are therefore found in similar local environment.

Another way to attain a proper description of electron states in plasmas is not to make an assumption of identical conditions (and identical level scheme) for all ions in plasma, but rather to account directly for the statistics of electron state perturbation by the near neighbor particles. Such a formalism, applicable to dilute as well as dense plasmas, has been proposed three decades ago. This is a so-called effective statistical weights (ESW) formalism, also known as an "occupation probabilities" formalism [7–12]. In its framework, the gradual elimination of a certain bound state in the ensemble of ions in plasma, say, with an increase in density, is described as the reduction of the ESW of that bound state relative to its statistical weight in an isolated ion. The ESW formalism in its original form [7,8] presents a powerful tool for plasma modeling. It allows to treat differently individual ions of the same ionization stage of the same element, according to the local micro-conditions at the locations of individual ions. (The same state can be bound in some ions and collectivized in the others.) This can be achieved neither in the traditional nor in the average-atom treatment. Despite its long history, the ESW formalism has not yet replaced the traditional "identical local environment" approach in the modeling of plasma bound-state population dynamics and plasma radiation. So far, the ESW formalism has only been utilized in the framework of the Opacity Project [13], for plasmas in local thermodynamic equilibrium. We are not aware of the ESW formalism being utilized for population kinetics modeling of any kind.

We note that the use of the bound-state ESWs alone does not provide, of course, an account for the variance of local micro-conditions. In some average-atom treatments (for example, XSN [9] and SCAALP [14]) as well as in MM model [15] the statistical weights of bound states are reduced towards the continuum limit, but still all the ions of the same element (and, in [15], of the same ionization stage) are assumed to have the same level structure. Rather, it is the detailed treatment of collectivization of bound states, in which the list of bound and collectivized states is allowed to differ between individual ions of the same element and ionization stage, that provides a possibility to construct a detailed kinetic model accounting for the variation of local micro-conditions between the locations of individual ions.

Our goal is the development of a kinetic model applicable to nonideal plasmas as well as to weakly coupled ones. We discard therefore the traditional assumption of an identical environment for all atoms (ions), and account for the statistics of electron state perturbation by neighbor particles. Thus, the ESW formalism must be incorporated into the model. Furthermore, we have found that the second traditional assumption—namely, that of only two types of electron states,—must also be revised. Indeed, there exists a third type of states, which are not yet free, but no longer bound to a single parent ion. These are the collectivized states. The collectivized states lie between the bound states and the free electron states, playing an important role in the electron state population dynamics. As we show below, the collectivized states can be described neither as free states nor as the states bound to a single parent ion, and must be considered as a separate, third type of states, along with the bound and the free electron states.

In the present paper we report a kinetic model developed in the framework of the present approach, and a time-dependent CR code based on it. We modify the basic notions of the free electron density and of the rate coefficient, and derive expressions for probabilities of collisional and radiative transitions between electron states. Examples of some test-case calculations for recombining carbon plasmas are given.

2. Present model

Here we present an approach to plasma modeling which is free from the traditional assumptions of identical local environment for all ions of a given charge and of two types of electron levels. We describe the three distinct types of electron states: the bound, the collectivized, and the free electron states. We consider the statistics of collectivization of electron states in plasma. The basis of the present approach has already been described in detail in Ref. [16], so in this section we provide a summary of the model.

The definition of each type of electron states is as follows.

- An electron in a positive-energy state is considered free.
- An electron in a negative-energy state, bound in a potential well of a single parent ion, is considered bound.

- An electron in a negative-energy state, which is free to move adiabatically between the potential wells of two or more ions, is considered collectivized.

Freedom of motion between the potential wells means that the motion is either overbarrier (adiabatic motion at negative energy, along the path(s) where the interionic barrier is sufficiently low), or tunneling on a time-scale shorter than the lifetime of this state with respect to all possible collisional and radiative transition channels together.

The collectivization of an electron states is governed by the local arrangement of perturbing particles around the parent ion, and thus any certain state is collectivized only in a fraction of ions in the ensemble. Therefore, we describe the collectivization of bound states statistically, using the ESW formalism. That is, in any individual ion an electron state q is either bound or collectivized, deterministically, according to the local arrangement of the surrounding perturber particles. Since the local conditions vary from ion to ion, in an ensemble of ions each state q is bound in a fraction ω_q of the ions, and collectivized in a fraction $1-\omega_q$ of the ions. For the bound fraction ω_q thus defined, the ESW $g_q^{[\mathrm{d}]}$ of the state q is given by

$$g_q^{[\mathrm{d}]} = \omega_q g_q^{[0]}, \tag{1}$$

where $g_q^{[0]}$ is the statistical weight of the state q in an isolated ion. As the plasma density decreases, $\omega_q \to 1$ and $g_q^{[\mathrm{d}]} \to g_q^{[0]}$. In the opposite limit of a very high density, $\omega_q \to 0$ and $g_q^{[\mathrm{d}]} \to 0$, so the state q becomes fully collectivized.

Thus, *in a single ion*, there are bound states, collectivized states, and free electron states. Of course, the spatial extent of the last two types is notably larger than the mean atomic volume. If a certain state is collectivized then all the states above it (i.e., with binding energies closer to zero) are obviously collectivized, too. So, in a single ion, the collectivized states are located above the bound states, and the free states are located above the collectivized ones. A state with zero binding energy is certainly an overbarrier state, and is fully collectivized (*in the ensemble* there is not a single ion in which this state remains bound, i.e., $\omega = 0$). All the lower-lying states, however, are collectivized in some ions and bound in other ions, so, in the ensemble of ions, all negative-energy states are partially collectivized, $0 < \omega < 1$.

The very high excited states are eliminated altogether in plasma by the binding energy reduction due to plasma polarization (screening). These states are moved into the positive-energy domain, and dissolved in the free-electron continuum. We stress the crucial difference between the screening effect and the collectivization effect. The collectivization is dominated by an arrangement of a few nearest perturber ions, and thus affects every individual ion differently. The screening, on the other hand, is essentially a collective phenomenon, involving many screening particles, and thus the binding energy reduction due to screening is practically the same in all ions of a given charge. In other words, in the ensemble of ions, there exists a boundary between the collectivized and the free states (and thus a certain state has the same binding energy in all ions), but there exists no boundary between the bound and collectivized states (and thus the same state is bound in one ion and collectivized in another one). Consequently, in plasmas the collectivized states do not form a band above the bound states, but rather coexist with the bound states throughout the negative-energy domain.

In atomic or ionic crystals, however, the collectivized states do form a conductivity band above the bound states domain (the latter being the valence band), and a well-defined boundary exists between the two. The present approach describes the change in an electron structure from plasma to condensed matter, as it accounts for the dependence of the near-ion distribution functions on the ion–ion coupling parameter

$$\Gamma_{\mathrm{ii}} = \frac{Z_{\mathrm{i}}^2 e^2}{a T_{\mathrm{i}}}, \tag{2}$$

where T_{i} is an ion temperature and

$$a = \left(\frac{4}{3}\pi N_{\mathrm{i}}\right)^{-1/3} \tag{3}$$

is a characteristic interionic distance. To follow the change in an electron-state structure let us consider an energy region in which, for given plasma parameters and composition, both the bound and the collectivized states are well-represented. That is, in the negative-energy domain we consider a region ΔE in which, for the states of a given element and ionization stage, neither ω nor $1-\omega$ is smaller than, say, 10^{-3}. In plasmas with $\Gamma_{\mathrm{ii}} \lesssim 1$ this region is broad and usually encompasses at least a few consecutive values of the optical-electron principal quantum number. This is due to the fact that the probability $P_0(R)$ to find no perturber ions within the distance R from the test ion in plasmas with $\Gamma_{\mathrm{ii}} \lesssim 1$ decreases from 0.999 to 10^{-3} over a broad range ΔR of R values [16]. (For ΔR, "broad" means comparable to a). An increase in Γ_{ii} produces narrowing of ΔR, and for $\Gamma_{\mathrm{ii}} \gg 1$ one finds $P_0(R)$ becoming increasingly step-like, dropping fast in the vicinity of a certain distance $R = a_1$, a_1 being comparable to a. Thus, as Γ_{ii} increases, the states collectivized by perturber ion(s) at the distance $R = a_1$ have $\omega \to 0$, while the deeper-lying states (that remain bound despite the presence of perturber ion(s) at the distance a_1) have $\omega \to 1$. For $\Gamma_{\mathrm{ii}} > 150$ plasma crystallizes [17], and $P_0(R)$ becomes effectively a step function (thermal and zero-oscillations can be neglected, as their amplitude in solids is much smaller than a). The boundary emerges then between the states which have $\omega = 0$ and form a conductivity band, and the lower-lying states which have $\omega = 1$, i.e., are fully bound.

As far as the notation of electron states in plasma ions is concerned, to denote a bound or a collectivized state we use the quantum numbers of the corresponding bound state of an isolated ion. Of course, some of these quantum numbers are no longer conserved in plasma ions. Such quantum numbers are used for the book-keeping purposes only; see, for example, the discussion of the orbital angular momentum conservation in Ref. [16]. The collectivized states are formed as superpositions of bound states localized at two or more adjacent ionic potential wells. A state spanning two similar potential wells is split into two states of slightly different energy, forming a doublet [18]. The total number of states is conserved, of course, since two bound states (each state confined to an individual well) form one doublet. Likewise, a state spanning N adjacent potential wells in plasma is split into N components and forms a narrow band, but still the total density of states is conserved. Thus, saying "a collectivized state q of the test ion" we in fact imply not the single state, but the narrow band of states located (along the energy axis) approximately where the bound state q used to be, and composed (at least as far as the contribution from the test-ion potential well is concerned) predominantly of the state q. The number of states *per ion* in such a band equals one if the original state q was non-degenerate. In the general case, it equals the original degeneracy g_q^0 of the state q in an isolated ion.

Now that the level structure is defined, the determination of the bound fractions and of the ESWs is tedious but straightforward. The details of ESW determination procedure are given in Ref. [16], and the neighbor-ion distribution functions, required for the determination of the ESWs, are presented in Ref. [19]. The main conclusions we have drawn from the ESW calculations are as follows:

- It is more accurate to approximate the perturbing potential by that of two (or even one) nearest neighbor ion(s) than to assume the uniformity of a local microfield at the parent ion location.
- One *must* take the effect of the next-nearest neighbor, i.e., the ion second-nearest to the test ion, into account for tunneling calculations.
- The ESW always decreases with density. However, at any given density, there are several distinct temperature effects that influence the ESWs, so the overall temperature dependence is often nontrivial.
- Both collectivization mechanisms actually play a part, and must be accounted for. The tunneling tends to dominate for low-lying states (principal quantum number $n = 1, 2, 3$), while overbarrier escape dominates for higher states. We have observed this effect for elements hydrogen through carbon, and this may persist in high-Z element plasmas. Overbarrier escape also takes over as the binding energy decreases due to changes in screening.

3. Redefinition of the basic quantities

In the present approach, there are three types of electron states instead of the traditional two, and furthermore any electron state q is bound in some ions and collectivized in the others. These features of the approach necessitate the redefinition of some basic physical quantities describing the plasma. Ionization stage populations N_Z, free electron density N_e, and rate coefficients $\langle \sigma_{ij} v \rangle$ must all be defined in a new way. In this Section we explain the physical basis of this redefinition. In the next Section we construct the quantitative kinetic model in the framework of the present approach. We note that populations and particle densities are given in units of cm^{-3}. Abundances, i.e. populations related to the total ion density, are dimensionless.

First of all, let us return to the physical picture of the levels of each type. As it follows from the definition of a collectivized state, it is populated and depopulated by tunneling and overbarrier motion in the time-dependent field of all the surrounding particles (which induces primarily the transitions between the adjacent energy levels; transitions involving large energy transfer are relatively rare events). That is, collectivized states are populated and depopulated much in the same way as the free-electron states. The collectivized states also resemble the free states as the electrons occupying the collectivized states participate in the screening, and (energy permitting) also in the inelastic collisions. Therefore, the generalized free electron density N_e is the sum of number densities of collectivized electrons N_c and of the positive-energy electrons N_f. That is,

$$N_e \equiv N_c + N_f. \tag{4}$$

Following the ESW formalism convention, we denote by N_q the population of the bound fraction of the state q, i.e., the number density of ions in which the state q is populated and bound. Number density of the ions in which the state q is populated and collectivized is included into the number density of the respective parent ions (i.e., the ions obtained after the removal of the collectivized electrons). Consequently, the electroneutrality constraint is given simply by

$$N_{\mathrm{e}} = \sum_{Z_{\mathrm{i}}} Z_{\mathrm{i}} N_{Z_{\mathrm{i}}}, \tag{5}$$

where

$$N_{Z_{\mathrm{i}}} \equiv \sum_{q \in Z_{\mathrm{i}}} N_q \tag{6}$$

is the total number density of the ions of the charge Z_{i}, evaluated according to the above rules. It is important to stress that the ESW values are evaluated self-consistently, with the free electron density and ionization stage populations determined following the definitions (4)–(6).

In the present approach the notion of a rate coefficient must be redefined, as well. Indeed, in the traditional approach the level scheme was assumed the same for all ions of a given charge, and therefore the $\langle \sigma_{ij} v \rangle$ averaging of the transition cross-section σ_{ij} with the incident electron velocity v was carried out over the incident electron velocity distribution only. In the framework of the present approach, however, all the ions are no longer assumed to have the same level scheme, so a double averaging must be carried out in order to determine $\langle \sigma_{ij} v \rangle$: it is necessary to average once over the electron velocity distribution and once over the ion ensemble composition. Consider, for example, an excitation from a bound state i. When the averaging over the ion ensemble is carried out, the rate coefficient splits into two contributions: a contribution from the ions in which the upper state j is also bound, and the contribution from ions in which the upper state j is collectivized. The first process does not change the number of bound electrons. The second process, however, converts one bound electron into a collectivized one. As we said, both the collectivized and the free state populations participate in the free electron density count (4), so the transition between a bound lower state and a collectivized upper state is, in fact, a second channel for *ionization*. The same applies to a photoexcitation process: such a process in the ions where the final (upper) state is collectivized provides a second channel for a photoionization. Of course, there exists also the usual bound-free ionization channel: an electron impact or a photon absorption can induce a transition from a bound initial state into a free-electron final state. It is important to notice that the collectivized states lie below the edge of the positive-energy free-electron domain, and therefore the bound-collectivized ionization from any state q requires a smaller energy investment than the usual bound-free ionization. Thus, there exists an obvious effect of the electron temperature T_{e} on the relative importance of the two channels.

There exist, of course, the inverse (reciprocal) processes for each of the processes mentioned above. The process inverse to the electron-impact transition from the bound lower state i to the collectivized upper state j is, of course, the electron-impact transition from the collectivized upper state j to the bound lower state i. This process provides the second channel for the 3-body recombination. The process inverse to the photoabsorption transition from i to j is the radiative transition from j to i. This provides the second channel for radiative recombination. Autoionization and dielectronic capture are not discussed in the present paper.

We note that there exists also a distinct effect of the ion temperature T_{i} (which is the temperature characterizing the *ion* velocity distribution) on the rate coefficients of electron-impact caused and photon-caused transitions. As we said above, decrease in T_{i} (i.e., increase in Γ_{ii}), even for a constant

T_e, results in changes to the ESWs of the bound states. The redefined excitation, ionization, and recombination rates all depend on the ESWs of the initial and final states, and are thus sensitive to the ion temperature. Below, we derive expressions for the redefined rate coefficients, probabilities, and rates, and illustrate the plasma composition sensitivity to T_i for a given value of T_e. By contrast, the traditional rate coefficients, probabilities, and rates of electron-impact caused and photon-caused transitions do not normally depend on the ion temperature.

Having thus redefined the basic quantities, we can now proceed with the construction of a detailed kinetic model in the framework of the present approach.

4. Kinetic model

Plasma composition, i.e., the populations N_q of all *bound* electron states in plasma, is traditionally found as a solution of the set of rate equations

$$\frac{\mathrm{d}}{\mathrm{d}t} N_q = \sum_{q' \neq q} \sum_{p} ({}^{p}W_{q'q} N_{q'} - {}^{p}W_{qq'} N_q) \tag{7}$$

for the given initial conditions. Here ${}^{p}W_{qq'}$ is the probability (in units of inverse time) for a transition process p from the state q into the state q' to occur in an ion in plasma under given conditions (ion density, free electron density, ion and electron temperature). q denotes a quantum state (usually, an ionic term) of a given ionization stage Z of a given chemical element. The summation over q' in the right-hand side of (7) is over all negative-energy states of all ionization stages of the given chemical element. The set of Eqs. (7) obviously observes the total ion number conservation

$$\sum_{q} \frac{\mathrm{d}}{\mathrm{d}t} N_q = 0.$$

The free electron density N_e, which enters explicitly some of the expressions for ${}^{p}W_{qq'}$, must be evaluated using the neutrality equation (5).

This method of determination of the plasma composition is valid in the framework of the present approach as well as in the framework of the traditional approach. However, now the set is incomplete, since it only describes the populations of the bound states. The populations of the collectivized states must be determined, too, in order to proceed. The rigorous solution to the problem of the plasma composition determination would be, therefore, to generalize the set of Eqs. (7) to include the collectivized states, too (but keeping only the bound states in the right-hand side of the neutrality Eqs. (5) and (6), as explained in the previous section). However, this is an exceedingly complicated technical problem, since the cross-sections for transitions between collectivized states would have to be evaluated. Even with the computers presently available the ensuing many-body time-dependent quantum-mechanical problems cannot be solved [20,28],[2] thus, such a complete description, although feasible in future, cannot at present be realized even for the simplest systems, e.g., hydrogen.

---

[2] We note that even for *bound* states, where the smaller spatial extent of the wavefunctions makes interaction with the spectator electrons much less important or outright negligible, the transition cross-section values are not easily determined, and their values are often the subject of substantial controversy. See, for example [20,28].

Fortunately, the relatively large spatial extent of the collectivized states, which makes the calculation of collectivized-collectivized and collectivized-free transition cross-sections such a formidable problem, also provides for their rapid equilibration with the positive-energy free-electron subsystem. As we said above, the collectivized states are populated and depopulated by tunneling and overbarrier motion of electrons in the time-dependent field of all the surrounding particles. That is the same way in which the free-electron states are populated and depopulated. It is therefore expected that the collectivized states reach thermodynamic equilibrium with the ground state of the next ionization stage and with the positive-energy free-electron subsystem on the time-scale of the free-electron Maxwellization. (Maxwellization was shown by Busquet [15] to occur even in the high-lying bound states, which have a significantly smaller spatial extent than the collectivized states.) The observation that the collectivized state populations equilibrate with the next ground state on the time-scale of the free-electron Maxwellization is important. Indeed, this removes the need to calculate the rates of all collectivized-collectivized, collectivized-free, and free-collectivized channels, thus making the plasma composition calculations in the framework of the present approach not much more complicated than they are in the traditional approximations. However, this is only true for the plasmas with Maxwellian free-electron energy distribution. In plasmas with non-Maxwellian electron energy distribution, detailed calculations of collectivized state populations are mandatory. We do not consider such situations in this paper, restricting ourselves to the plasmas with approximately Maxwellian distribution.

To complete the physical picture, we must now determine the cross-sections of bound–collectivized and collectivized–bound transitions. As we already said, the collectivized states are made up of the superpositions of bound states, and not of the positive-energy states. Thus, the cross-sections of bound–collectivized transitions are closely related to the cross-sections of bound–bound transitions, and not to the cross-sections of the bound-free transitions. To see this, let us consider a slightly more detailed picture. Consider a collisional or radiative process p producing a bound–collectivized transition. The transition matrix element ${}^{p}M$ is determined by the overlap of the wavefunctions of the initial and final states. Here, although the wavefunction $\Phi_{q'}(\mathbf{r})$ of the final (collectivized) state q' spans several potential wells, the wavefunction $\Psi_q(\mathbf{r}-\mathbf{r}_\mathrm{i})$ of the initial state q is bound in a single ionic potential well, centered at $\mathbf{r}_\mathrm{i}$, and it is only the overlap over this well that contributes to the transition matrix element ${}^{p}M_{qq'}$. Thus, only the spatial integral over the potential well of a single ion appears in the expression

$${}^{p}M_{qq'} = \int \Phi^{*}_{q'}(\mathbf{r})\hat{O}_p(\mathbf{r})\Psi_q(\mathbf{r}-\mathbf{r}_\mathrm{i})\,\mathrm{d}\mathbf{r} \tag{8}$$

for the matrix element, where $\hat{O}_p(\mathbf{r})$ is the transition operator. In other words, the integration in (8) can be restricted to the domain $|\mathbf{r}-\mathbf{r}_\mathrm{i}| \lesssim a$, where a is the mean interionic distance, without a significant loss of accuracy. Now, as explained above, in any given ion each collectivized state is composed predominantly of a single bound state (which quantum numbers q' were used to denote the collectivized state in the first place). We denote the wavefunction of this original bound state by $\Psi_{q'}(\mathbf{r}-\mathbf{r}_\mathrm{i})$. Then, for $|\mathbf{r}-\mathbf{r}_i| \lesssim a$,

$$\Phi_{q'\alpha}(\mathbf{r}) \approx N^{-1/2}\Psi_{q'}(\mathbf{r}-\mathbf{r}_\mathrm{i})\mathrm{e}^{\mathrm{i}\varphi_\alpha}, \tag{9}$$

where N is the number of potential wells the wavefunction $\Phi_{q'}(\mathbf{r})$ spans, $\alpha = 1\ldots N$ is the index of a component of the state $\Phi_{q'}$, and $\mathrm{e}^{\mathrm{i}\varphi_\alpha}$ is a constant phase factor. The total cross-section ${}^{p}\sigma^{[\mathrm{bc}]}_{q\to q'}$ of a transition from the bound state q into the collectivized state q' is given by

$$^{p}\sigma^{[\mathrm{bc}]}_{q\to q'} = C_p \sum_{\alpha=1}^{N} |^{p}M_{qq'\alpha}|^2 \approx C_p \left| \int \Psi^*_{q'}(\mathbf{r}-\mathbf{r}_\mathrm{i})\hat{O}_p(\mathbf{r})\Psi_q(\mathbf{r}-\mathbf{r}_i)\,\mathrm{d}\mathbf{r} \right|^2,$$

where the factor C_p depends on the type of process and on projectile parameters, but not on the initial and final state involved. The expression obtained on the right-hand side is identical to the expression for the cross-section $^{p}\sigma^{[\mathrm{bb}]}_{q\to q'}$ of a *bound–bound* transition $q \to q'$ in an *isolated* ion. Thus, one can approximate the probabilities for bound–collectivized transitions by the probabilities of the corresponding bound–bound transitions,

$$^{p}\sigma^{[\mathrm{bc}]}_{q\to q'} \approx {}^{p}\sigma^{[\mathrm{bb}]}_{q\to q'}. \tag{10}$$

Exactly the same argument applies to the Einstein coefficients, too. Cross-sections for collectivized–bound transitions are determined in the same way as the bound–collectivized cross-sections

$$^{p}\sigma^{[\mathrm{cb}]}_{q'\to q} \approx {}^{p}\sigma^{[\mathrm{bb}]}_{q'\to q}. \tag{11}$$

We return to probabilities of radiative processes and to the discussion of the detailed balance later in this section.

It is important to note here that expression (9) is only approximate, and therefore expressions (10) and (11) provide only an approximate equality and certainly not an exact one. In the course of the future work, we hope to improve the description even further by introducing the cross-sections $^{p}\sigma^{[\mathrm{bc}]}_{q\to q'}$ for the bound–collectivized transitions that are not necessarily equal to the cross-sections $^{p}\sigma^{[\mathrm{bb}]}_{q\to q'}$ of the corresponding bound–bound transitions. This can be especially useful for detailed spectroscopic modeling, as the upper state q' can be characterized by a definite value of orbital and/or total angular momentum. An orbital momentum can still be a good quantum number for the bound fraction of the state q' (i.e., in the ions where the state q' is not collectivized), but it is probably not a good quantum number in the ions where the state q' is perturbed strongly enough to be collectivized. Then $^{p}\sigma^{[\mathrm{bc}]}_{q\to q'}$ can, in principle, be recalculated to include at least the potential of the near-neighbor ion(s) in the Hamiltonian, while $^{p}\sigma^{[\mathrm{bb}]}_{q\to q'}$ needs no amendment. However, at the present stage of the work we use the expressions (10) and (11) for all bound–collectivized and collectivized–bound transitions.

Now, using the rules introduced in the previous section and the treatment of the collectivized states introduced above, let us formulate the quantitative kinetic model. First, we consider the electron impact excitation. Only the excitation from a bound state must be considered. Indeed, in any *individual* ion there are bound states, collectivized states above them, and free electron states above the collectivized ones. Thus, there can be no bound states above a collectivized state in a given ion, and an excitation from a collectivized state can only bring an electron into another collectivized state. The collectivized state populations are known anyway, due to their rapid equilibration with the free electron subsystem, so the collectivized–collectivized transitions need not be considered. We thus only consider the bound–bound excitation (which is the true excitation process) and the bound–collectivized transitions (which are in fact ionization rather than excitation events).

Whenever in an individual ion a certain energy level is bound, all the lower levels are bound, too. The conditional probability for an upper level j to be bound, in a given ion in which the lower level

i is bound, is thus ω_j/ω_i. Consequently, averaging over an ensemble of *ions* in the state i results in the additional factor ω_j/ω_i for the redefined excitation rate coefficient. That is,

$$\langle {}^{\mathrm{ex}}\sigma_{ij}v\rangle^{[\mathrm{d}]} = \langle {}^{\mathrm{ex}}\sigma_{ij}v\rangle^{[0]}\,\frac{\omega_j}{\omega_i}.$$

Here ${}^{\mathrm{ex}}\sigma_{ij}$ is the excitation cross-section for an isolated ion, and v is the incident free electron velocity. The angular brackets $\langle\sigma v\rangle^{[\mathrm{d}]}$ denote the redefined rate coefficient, obtained by averaging over *both* the ensembles of the ions and of the free electrons. The angular brackets $\langle\sigma v\rangle^{[0]}$ denote the traditional rate coefficient, obtained by averaging over the free-electron distribution only, assuming both levels i and j are bound. The collisional excitation probability in the present approach

$${}^{\mathrm{ex}}W_{ij}^{[\mathrm{d}]} = N_{\mathrm{e}}\langle {}^{\mathrm{ex}}\sigma_{ij}v\rangle^{[\mathrm{d}]},$$

is thus related to the traditional collisional excitation probability

$${}^{\mathrm{ex}}W_{ij}^{[0]} = N_{\mathrm{e}}\langle {}^{\mathrm{ex}}\sigma_{ij}v\rangle^{[0]}$$

by

$${}^{\mathrm{ex}}W_{ij}^{[\mathrm{d}]} = {}^{\mathrm{ex}}W_{ij}^{[0]}\,\frac{\omega_j}{\omega_i}. \tag{12}$$

The probability that the level j is *collectivized*, whereas the level i is bound, is $1-\omega_j/\omega_i$. The respective fraction of the excitation probability,

$${}^{\mathrm{ex}}W_{ij}^{[\mathrm{c}]} = {}^{\mathrm{ex}}W_{ij}^{[0]}\left(1-\frac{\omega_j}{\omega_i}\right), \tag{13}$$

corresponds to ionization and contributes to the population of the *parent* state of the state j.

For the deexcitation from the level j to i, whenever j is bound i is also bound. Thus, the deexcitation rate coefficient and the deexcitation probability in the present approach are not modified:

$$\langle {}^{\mathrm{dx}}\sigma_{ij}v\rangle^{[\mathrm{d}]} = \langle {}^{\mathrm{dx}}\sigma_{ij}v\rangle^{[0]},$$

$${}^{\mathrm{dx}}W_{ji}^{[\mathrm{d}]} = {}^{\mathrm{dx}}W_{ji}^{[0]}. \tag{14}$$

The probability of the photon-induced excitation (i.e., photoabsorption) in the present approach, ${}^{\mathrm{phab}}W_{ij}^{[\mathrm{d}]}$, can be found in exactly the same way as the electron-impact excitation probability above. We find

$${}^{\mathrm{phab}}W_{ij}^{[\mathrm{d}]} = {}^{\mathrm{phab}}W_{ij}^{[0]}\,\frac{\omega_j}{\omega_i}, \tag{15}$$

where ${}^{\mathrm{phab}}W_{ij}^{[0]}$ is the traditional photoabsorption probability. Like the electron-impact deexcitation probability, the probability A_{ji} of the spontaneous radiative decay (the Einstein coefficient) is not modified. Thus

$$A_{ji}^{[\mathrm{d}]} = A_{ji}. \tag{16}$$

The same is true for the induced radiative decay probability ${}^{\mathrm{phdx}}W_{ji}^{[\mathrm{d}]}$. Thus,

$${}^{\mathrm{phdx}}W_{ji}^{[\mathrm{d}]} = {}^{\mathrm{phdx}}W_{ji}^{[0]}. \tag{17}$$

Collisional ionization probability in the present approach is introduced as follows. When a given state is bound, its parent state is certainly bound, too. Therefore, the probability of the direct (bound-free) ionization ${}^{\mathrm{io}}W_{i_Z j_{Z+1}}$ is not modified. However, the probability of ionization from a state i_Z into a state j_{Z+1} is increased by the contributions ${}^{\mathrm{ex}}W_{ik}^{[\mathrm{c}]}$ of the excitation from i_Z into the collectivized fractions of the higher states k_Z whose parent is j_{Z+1}. Thus, in the present approach

$$ {}^{\mathrm{io}}W_{i_Z j_{Z+1}}^{[\mathrm{d}]} = {}^{\mathrm{io}}W_{i_Z j_{Z+1}}^{[0]} + \sum_{k_Z > i_Z} {}^{\mathrm{ex}}W_{ik}^{[0]} \left(1 - \frac{\omega_{k_Z}}{\omega_{i_Z}}\right) \delta\ (\mathrm{parent}\ \{k_Z\}, j_{Z+1}), \tag{18} $$

where δ is the Kronecker delta symbol, and the sum is over all the levels k_Z above the level i_Z in the charge state Z. We would like to emphasize the two important effects described here. First, the existence of bound–collectivized ionization alters the threshold energy at which a projectile (a photon or an electron) is predicted to cause ionization from a given state. This threshold energy becomes lowered stronger than predicted accounting for the plasma polarization alone, and smeared. Second, a bound–collectivized ionization process can populate a state j_{Z+1} which is not a parent state of an initial state i_Z. Indeed, an excitation from i_Z into a collectivized state k_Z populates a state j_{Z+1} which is a parent state of k_Z but not necessarily a parent state of i_Z. These two effects are overlooked in the traditional approach. We note that these effects take place in all plasmas and not only in the dense ones. However, their relative importance is higher in dense plasmas than in dilute ones.

Photoionization is described similarly to the electron-impact ionization. We find

$$ {}^{\mathrm{phio}}W_{i_Z j_{Z+1}}^{[\mathrm{d}]} = {}^{\mathrm{phio}}W_{i_Z j_{Z+1}}^{[0]} + \sum_{k_Z > i_Z} {}^{\mathrm{phab}}W_{ik}^{[0]} \left(1 - \frac{\omega_{k_Z}}{\omega_{i_Z}}\right) \delta\ (\mathrm{parent}\ \{k_Z\}, j_{Z+1}), \tag{19} $$

where ${}^{\mathrm{phio}}W_{i_Z j_{Z+1}}^{[\mathrm{d}]}$ and ${}^{\mathrm{phio}}W_{i_Z j_{Z+1}}^{[0]}$ are photoionization probabilities in the present approach and in the traditional approach, respectively.

The probability of the 3-body recombination ${}^{3\mathrm{br}}W_{j_{Z+1} i_Z}^{[\mathrm{d}]}$ from j_{Z+1} into i_Z acquires a factor $\omega_{i_Z}/\omega_{j_{Z+1}}$, since the recombination is only viewed to occur when the final state i_Z is not collectivized (given the initial state j_{Z+1} is not collectivized). Thus the free-bound contribution to ${}^{3\mathrm{br}}W_{j_{Z+1} i_Z}^{[\mathrm{d}]}$ is

$$ {}^{3\mathrm{br(fb)}}W_{j_{Z+1} i_Z}^{[\mathrm{d}]} = {}^{3\mathrm{br}}W_{j_{Z+1} i_Z}^{[0]} \frac{\omega_{i_Z}}{\omega_{j_{Z+1}}}. $$

However, the probability of the 3-body recombination from j_{Z+1} into i_Z is increased by the de-excitation into i_Z from the collectivized higher-lying states k_Z for which j_{Z+1} is the parent. The collectivized states of Z are, as we said, in equilibrium with the free electron subsystem. We therefore *approximate* the population $N_{k_Z}^{[\mathrm{c}]}$ of the *collectivized fraction* of the state k_Z by the modified Saha relation

$$ N_{k_Z}^{[\mathrm{c}]} = N_{j_{Z+1}} \frac{N_{\mathrm{e}}}{C_{\mathrm{Saha}}} \frac{(1 - \omega_{k_Z})}{\omega_{j_{Z+1}}} \frac{g_{k_Z}^{[0]}}{g_{j_{Z+1}}^{[0]}} \exp\left(\frac{E_{j_{Z+1}} - E_{k_Z}}{T_{\mathrm{e}}}\right), \tag{20} $$

where

$$ C_{\mathrm{Saha}} = 2\left(\frac{2\pi m_{\mathrm{e}} T_{\mathrm{e}}}{h^2}\right)^{3/2}, \tag{21} $$

and $E_{j_{Z+1}} - E_{k_Z}$ is the binding energy of the state k_Z relative to its parent state j_{Z+1}. (We note that the binding energy depends on plasma parameters due to the plasma polarization effect.) The probability that deexcitation from collectivized state k_Z into a lower state i_Z results in a recombination is, by definition, given by the probability P to find i_Z bound when k_Z is collectivized. It is easy to see that

$$P = \frac{\omega_{i_Z} - \omega_{k_Z}}{1 - \omega_{k_Z}}.$$

Thus, for the rate in a collectivized–bound channel of the 3-body recombination we find

$$N_{j_{Z+1}}\,{}^{3\mathrm{br(cb)}}W^{[\mathrm{d}]}_{j_{Z+1} i_Z} = N^{[\mathrm{c}]\,\mathrm{dx}}_{k_Z} W^{[0]}_{k_Z i_Z} P$$

$$= N_{j_{Z+1}} \frac{N_\mathrm{e}}{C_\mathrm{Saha}} \frac{(\omega_{i_Z} - \omega_{k_Z})}{\omega_{j_{Z+1}}} \frac{g^{[0]}_{k_Z}}{g^{[0]}_{j_{Z+1}}} \exp\left(\frac{E_{j_{Z+1}} - E_{k_Z}}{T_\mathrm{e}}\right)^{\mathrm{dx}} W^{[0]}_{k_Z i_Z}.$$

Therefore, the total 3-body recombination probability (the sum of the free-bound and the collectivized–bound channels) is given by

$$ {}^{3\mathrm{br}}W^{[\mathrm{d}]}_{j_{Z+1} i_Z} = {}^{3\mathrm{br}}W^{[0]}_{j_{Z+1} i_Z} \frac{\omega_{i_Z}}{\omega_{j_{Z+1}}} + \frac{N_\mathrm{e}}{C_\mathrm{Saha}} \sum_{k_Z > i_Z} {}^{\mathrm{dx}}W^{[0]}_{ki} \frac{(\omega_{i_Z} - \omega_{k_Z}) g^{[0]}_{k_Z}}{\omega_{j_{Z+1}} g^{[0]}_{j_{Z+1}}} \exp\left(\frac{E_{j_{Z+1}} - E_{k_Z}}{T_\mathrm{e}}\right) \delta\,(\mathrm{parent}\{k_Z\}, j_{Z+1}). \tag{22}$$

Likewise, the probability of the spontaneous radiative recombination, ${}^{\mathrm{rr}}W^{[\mathrm{d}]}$, is described by the expression

$$ {}^{\mathrm{rr}}W^{[\mathrm{d}]}_{j_{Z+1} i_Z} = {}^{\mathrm{rr}}W^{[0]}_{j_{Z+1} i_Z} \frac{\omega_{i_Z}}{\omega_{j_{Z+1}}} + \frac{N_\mathrm{e}}{C_\mathrm{Saha}} \sum_{k_Z > i_Z} A_{ki} \frac{(\omega_{i_Z} - \omega_{k_Z}) g^{[0]}_{k_Z}}{\omega_{j_{Z+1}} g^{[0]}_{j_{Z+1}}} \exp\left(\frac{E_{j_{Z+1}} - E_{k_Z}}{T_\mathrm{e}}\right) \delta\,(\mathrm{parent}\{k_Z\}, j_{Z+1}) \tag{23}$$

which is similar to (22), with the replacement of ${}^{3\mathrm{br}}W$ by ${}^{\mathrm{rr}}W$ and ${}^{\mathrm{dx}}W^{[0]}$ by A. Analogously, the probability of induced radiative recombination ${}^{\mathrm{irr}}W^{[\mathrm{d}]}$ is given by

$$ {}^{\mathrm{irr}}W^{[\mathrm{d}]}_{j_{Z+1} i_Z} = {}^{\mathrm{irr}}W^{[0]}_{j_{Z+1} i_Z} \frac{\omega_{i_Z}}{\omega_{j_{Z+1}}} + \frac{N_\mathrm{e}}{C_\mathrm{Saha}} \sum_{k_Z > i_Z} {}^{\mathrm{phdx}}W^{[0]}_{ki} \frac{(\omega_{i_Z} - \omega_{k_Z}) g^{[0]}_{k_Z}}{\omega_{j_{Z+1}} g^{[0]}_{j_{Z+1}}} \exp\left(\frac{E_{j_{Z+1}} - E_{k_Z}}{T_\mathrm{e}}\right) \delta\,(\mathrm{parent}\{k_Z\}, j_{Z+1}). \tag{24}$$

In the case of fractional parentage for k_Z, only the *lowest-energy* parent state must be taken. The Kronecker delta in expressions (18), (19), (22)–(24) is then multiplied by the value of the respective fractional-parentage coefficient. Tunneling escape of the optical electron producing a higher-energy parent state is exponentially suppressed (see Ref. [21]), therefore the collectivization of the state k_Z implies that the lowest-energy parent state is produced.

When the above expressions are incorporated in the computer codes, the following precaution must be taken. The ω values can easily become very small, especially for high energy levels of low ionization stages. The ω values smaller than the minimal representable positive real are represented by a computer as an exact zero. Thus, the ratio ω_j/ω_i of bound fractions of the upper state j and the lower state i can become 0/0 numerically. Analytically, ω_j/ω_i poses no problem regardless of the values of ω_j and ω_i, since $0 \leqslant \omega_j \leqslant \omega_i \leqslant 1$ (where $\omega_j = \omega_i$ if and only if $\omega_j = \omega_i = 1$), which implies $0 \leqslant \omega_j/\omega_i \leqslant 1$. In the limit $\omega \to 0$ the dependence of ω on the binding energy becomes extremely strong, so one should expect the ratio ω_j/ω_i to approach zero asymptotically whenever $\omega_i \to 0$. Therefore, the correct limit is

$$\lim_{\omega_i \to 0} \{\omega_j/\omega_i\} = 0.$$

To summarize, all the transition probabilities and rates of all the relevant processes: electron-impact induced transitions, spontaneous and induced radiative transitions,—can be inferred using the book-keeping rules described in the previous section and the probabilities expressed, as explained above, via the cross-sections for bound–bound and bound-free transitions that are available in literature (see e.g. Refs. [22–24]). The approximate equalities (10) and (20), incorporated in the present kinetic model, represent quantitatively the two basic approximations made, namely, that of transition cross-section invariance under collectivization of upper state, and that of equilibrium between collectivized and free states. Expressions (11)–(19), (22)–(24) follow from (10) and (20), with no additional approximations made at any stage.

The above expressions obey the detailed balance requirement. For ionization and recombination, the bound–free (free–bound) channel and every bound–collectivized (collectivized–bound) channel balances individually. The equilibrium composition is given by the modified Saha–Boltzmann relations

$$\frac{N_{i_Z}}{N_{j_{Z+1}}} = \frac{N_{\mathrm{e}}}{C_{\mathrm{Saha}}} \frac{\omega_{i_Z}}{\omega_{j_{Z+1}}} \frac{g_{i_Z}^{[0]}}{g_{j_{Z+1}}^{[0]}} \exp\left(\frac{E_{j_{Z+1}} - E_{i_Z}}{T_{\mathrm{e}}}\right), \tag{25}$$

$$\frac{N_{i_Z}}{N_{j_Z}} = \frac{\omega_{i_Z}}{\omega_{j_Z}} \frac{g_{i_Z}^{[0]}}{g_{j_Z}^{[0]}} \exp\left(\frac{E_{j_Z} - E_{i_Z}}{T_{\mathrm{e}}}\right), \tag{26}$$

consistent with Eq. (20). We stress that $E_{j_{Z+1}} - E_{i_Z}$ and ω_{i_Z} are functions of plasma parameters. The approximations made allowed us, therefore, to obtain the equilibrium plasma composition without guessing or deriving first the expression for Helmholtz free energy F. This approach is different from the traditional one. Indeed, one usually makes approximations on the functional form of the free energy, and then finds the equilibrium composition $\mathbf{N}$ by minimizing F $(\mathbf{N}, T)$ with respect to population balance (see e.g. Ref. [25]). Here, an opposite approach is chosen. We have found the equilibrium composition $\mathbf{N}$ (N_{tot}, T), where N_{tot} is the total ion density. Then, knowing $\mathbf{N}$ (N_{tot}, T), it is possible to determine the corresponding F which is minimized by $\mathbf{N}$ (N_{tot}, T), at least up to some global terms which do not depend on composition. This procedure will be described separately.

5. Calculation examples

The CR code realizing the present model has been built on the basis of traditional-approach time-dependent CR code [26] developed and utilized routinely at the Plasma Laboratory of the

Weizmann Institute of Science. The code uses atomic databases common for all the codes of the Laboratory. The details on the databases are given, e.g., in Ref. [24].

First we present as an example the results of calculations carried out for carbon plasma. The case of a fully ionized carbon plasma recombining at constant temperature ($T_e = T_i = 2$ eV) and constant total ion density $N_{tot} = 10^{19}$ cm^{-3} was considered. This case was originally used for a code comparison workshop, see Ref. [27]. In our calculations, the list of energy levels included 128 low-lying terms (20 for C I, 16 for C II, 44 for C III, 20 for C IV, 21 for C V, 6 n-states for C VI, and a bare nucleus C VII), followed by the Rydberg levels of the respective charge states ($n = 4$–12 for C I, $n = 5$–14 for C II, $n = 6$–19 for C III, $n = 7$–21 for C IV, $n = 5$–25 for C V, $n = 7$–27 for C VI). Thus, a total of 218 distinct electron energy levels, with their respective degeneracies, were considered.

During every time step Δt the set of 218 equations (7) was solved numerically using the values of transition probabilities evaluated at the beginning of that step. At the beginning of every step the free electron density, the binding energies, the bound fractions, and the transition probabilities were updated in accord with the current level populations. The time step Δt was increased according to the exponential law, starting with 10^{-20} s and incrementing Δt by a factor of 1.2 every time. Tests showed that the values of Δt were small enough for the calculation results to be practically independent on Δt.

For the purpose of comparison with the results of the present approach, we have conducted calculations in the framework of the traditional approach. We would like to stress the fact that the present kinetic model can be reduced to the traditional model by taking $\omega \equiv 1$ for all the levels not destroyed by plasma polarization (or, in general terms of the traditional method, by continuum lowering). Thus, any CR code written in the framework of the present approach can also be utilized as a traditional-model CR code. Here, for comparison, we present the calculation results obtained in the traditional approach using an ion sphere model for continuum lowering (see Section 7.3 of Ref. [22]). It gives the continuum lowering value ΔI_Z for an ion of a charge Z as

$$\Delta I_Z = \frac{3}{2}(Z+1)\left(\frac{4}{3}\pi N_{tot}\right)^{1/3} a_0 Ry,$$

where a_0 is Bohr radius and Ry is one Rydberg.

Fig. 1 shows the calculated abundances of carbon ionization stages from helium-like to neutral. Fig. 2 shows the calculated abundances of the ground states of those ionization stages. One can see the significant differences in predictions of the present and the traditional model. In particular, substantial difference in the predicted rates of a 3-body recombination becomes apparent from Fig. 1. The successively lower ionization stages of carbon are predicted in the traditional model to become populated at substantially later times than in the present model. The discrepancies in population time-scales between the traditional and the present model are shown by arrows in Fig. 1 for C III and C IV. We note that the account for the 3-body recombination in the traditional approach is inherently problematic. This is due to the fact that the 3-body recombination proceeds predominantly into the highest bound states, so different choices of a model for continuum lowering ΔI_Z produce different values of the highest available principle quantum number, which results in significant ambiguity in the predicted 3-body recombination rates in the traditional approach. By contrast, the present approach, accounting for the level collectivization, produces unambiguous predictions for the 3-body recombination rates.

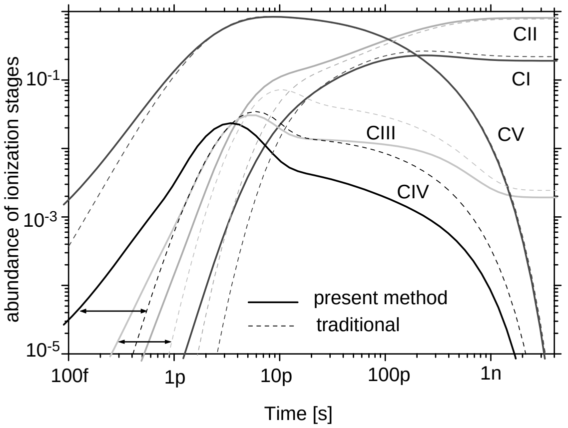

Fig. 1. Time-dependent abundances of the five lower ionization stages of carbon.

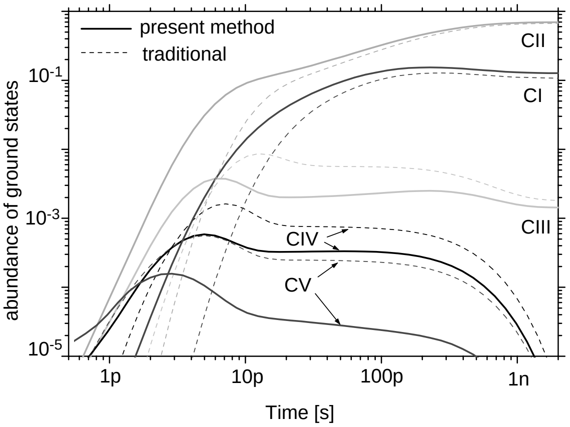

Fig. 2. Time-dependent abundances of the ground states of the five lower ionization stages of carbon.

As recombination proceeds, there is a significant population accumulation (over 80% of the total population) in the metastable state of C V, while the ground state of C V is only weakly populated, compare Figs. 1 and 2. The "recombination bottleneck" produced by the metastable state of C V is rather model-independent, and the predictions of both models considered for the total C V abundance converge to within 1% of each-other at the times approaching 10 ps. However, the predictions for the C V ground state abundance differ by as much as an order of magnitude at $t \geqslant 10$ ps. Prior to the arrival at the steady-state composition, significant differences between the predictions of the present and the traditional model are also observed in the abundances of the lower ionization stages of carbon and in the abundances of the respective ground states.

The present model, in comparison to the traditional one, modifies the free electron density and the rates of bound–bound and free–bound transitions, and introduces new collectivized–bound channels for the population and depopulation of the bound states. Both of these factors (modification of the existing channels, and introduction of the new ones) contribute to the differences in the predicted rates of kinetic processes. To determine the relative importance of the new channels, we have compared, for the carbon recombination case above, the partial rates of population of several bound states in bound–bound, collectivized–bound, and free–bound processes. In Fig. 3 we present the comparison results for the $2s^23d$ ^2D term of C II and for 2s4p ^3P, 2p3s ^3P, and 2s3p ^3P terms of C III. The 4 terms considered have, at $t = 10$ fs, bound fractions of 0.74, 0.80, 0.89, and 0.99, respectively. As the recombination progresses, the bound fractions increase monotonously, at $t = 10$ ns reaching 0.973, 0.984, 0.992, and 0.999, respectively. Thus, all 4 levels (terms) are predominantly bound throughout the time interval considered. Total rates of bound–bound, collectivized–bound, and free–bound transitions into each of the 4 levels were considered, summed over all contributing levels. The ratio between the total collectivized–bound and the total bound–bound rate is shown in Fig. 3 for each of the 4 levels. Total rates of the free–bound transitions were found to be significantly smaller than both the collectivized–bound and the bound–bound rates, and are not shown. As one can see, the collectivized–bound channels prove to be important and sometimes dominant in populating the levels shown, especially at earlier times when these levels are just becoming populated. We note

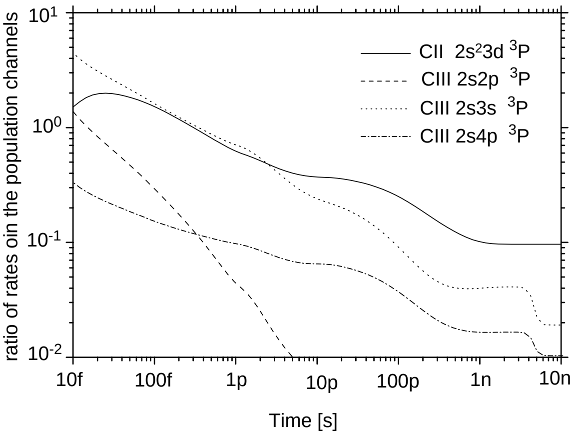

Fig. 3. Ratio of total rate in all collectivized–bound channels populating the given state to the total rate in all bound–bound channels populating the same state, for four states of carbon.

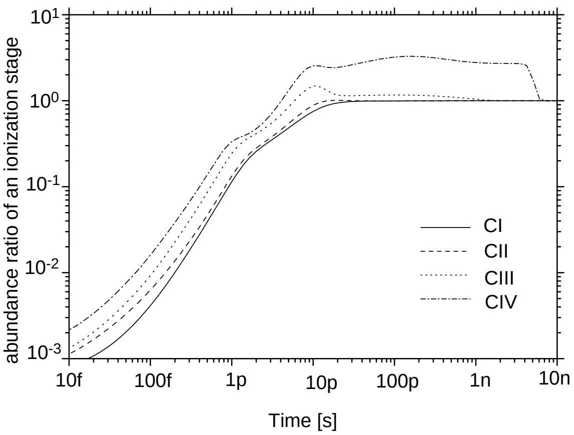

Fig. 4. Time-dependent ratio of carbon ionization stage abundance at ($T_i = 1$ eV, $T_e = 2$ eV) to the abundance of the same ionization stage at $T_i = T_e = 2$ eV, for lithium-, beryllium-, boron-like, and neutral carbon. For both T_i values the calculations are performed in the present approach.

that all 4 levels show appreciable abundances (about 10^{-6} or higher) for t between 0.3 ps and 2 ns, and the CII $2s^2 3d\,^2D$ level also at later times. The relative importance of the two types of channels differs, of course, for different levels. However, there is no strong decrease in the importance of collectivized–bound channels with an increase in the binding energy (that is, for deeper-lying levels) as one might have expected.

Present model predicts the dependence of the plasma composition on the ion temperature. Fig. 4 illustrates this result. For the recombining carbon case discussed above, it shows the ratios of the abundances of C I–C IV ionization stages evaluated for $T_i = 1$ eV to the same abundances for $T_i = 2$ eV. (The latter abundances are shown in Fig. 1 above.) One can see, indeed, a substantial dependence of the transient plasma composition on T_i for given T_e and N_{tot}.

6. Summary

We developed an approach for the description of plasma collisional-radiative kinetics, free from the oversimplifying assumptions of (1) identical local environment and identical level scheme for all ions of a given ionization stage and (2) two types of electron states. The definitions have been given for the three distinct types of electron states, and an appropriate level scheme was developed based on the statistics of local micro-conditions. Both individual and collective effects of the surrounding electrons and ions have been accounted for. The statistics of electron state collectivization in the ensemble of ions was incorporated into the present approach by means of the effective statistical weights formalism. The spatial distributions of the *two* nearest neighbor ions around a given one were determined in Ref. [19]. Using the distributions found, the accurate expressions for the ESW values in the framework of the present approach were found in Ref. [16].

The present approach requires the redefinition of the basic quantities such as free electron density, ionization stage populations, and rate coefficients. The redefined quantities are introduced. This allowed us to formulate a detailed kinetic model, and to determine the probabilities and rates. We have demonstrated that an additional, second type of ionization and recombination channels becomes important in dense plasmas. These channels involve excitation and deexcitation between a lower bound state and an upper collectivized state. The recombination channels of the second type were shown to facilitate significantly the relaxation of ionization-stage composition in rapidly cooling dense plasmas. For a recombining plasma, a direct comparison has shown that the collectivized–bound populating rates can be comparable or even larger than both the bound–bound and free–bound populating rates for the same states. We have also demonstrated that the probabilities of main kinetic processes in plasmas depend on the ion temperature. This effect is caused by the ion-temperature dependence of the surrounding-ion spatial distribution that determines the ESW values.

We have found that, in the kinetic model developed, the probabilities of all the kinetic processes can be expressed via the cross-sections for transitions in *isolated* ions, available in literature, and the ESW values derived in Ref. [16]. This fortunate circumstance allowed to utilize the existing cross-section databases for the construction of a CR code realizing the present kinetic model. The nonequilibrium time-dependent CR code has been developed, and examples of calculations are presented here.

Acknowledgements

The work has been supported by German–Israeli Project Cooperation on Future-Oriented Topics, grant DIP-C 7.2, and, in part, by Sandia National Laboratories (USA) and the Israeli Science Foundation.

References

[1] Lee RW, editor. Proceedings of RPHDM-2000 workshop. JQSRT 2001;71:107–760.
[2] Lee RW, editor. Proceedings of RPHDM-2002 workshop. JQSRT, this issue.
[3] More RM. Adv At Mol Phys 1985;21:305–59.
[4] Liberman DA. Phys Rev B 1979;20:4981–9.
[5] Liberman D. JQSRT 1982;27:335–9.
[6] Liberman D, Albritton J. JQSRT 1995;53:729–33.
[7] Gündel H. Beitr Plasmaphys 1970;10:455–67.
[8] Gündel H. Beitr Plasmaphys 1971;11:1–12.
[9] Zimmerman GB, More RM. JQSRT 1980;23:517–22.
[10] Fortov VE, Yakubov LT. Physics of nonideal plasma. New York: Hemisphere Publ., 1990.
[11] Däppen W, Anderson L, Mihalas D. Astrophys J 1987;319:195–206.
[12] Hummer DG, Mihalas D. Astrophys J 1988;331:794–814.
[13] Seaton MJ, editor. The opacity project, vol. 1. Bristol: IOP Publ., 1995.
[14] Faussurier G, Blancard C, Berthier E. Phys Rev E 2001;63:026401-1–13.
[15] Busquet M. Phys Rev A 1982;25:2302–23.
[16] Fisher DV, Maron Y. Eur Phys J D 2002;18:93–111.
[17] Hansen JP, McDonald IRM. Theory of simple liquids. London: Academic Press, 1976.
[18] Landau LD, Lifshitz EM. Quantum mechanics (non-relativistic theory), 3rd ed. New York: Butterworth-Heinemann Publ., 1997.

[19] Fisher DV, Maron Y. Eur Phys J D 2001;14:349–59.
[20] Hegazy, et al. JQSRT;to appear.
[21] Fisher DV, Maron Y, Pitaevskii LP. Phys Rev A 1998;58:2214–24.
[22] Griem HR. Principles of plasma spectroscopy. Cambridge: Cambridge University Press, 1997.
[23] Sobel'man II, Vainshtein LA, Yukov EA. Excitation of atoms and broadening of spectral lines. Heidelberg: Springer, 1995.
[24] Ralchenko YuV, Maron Y. JQSRT 2001;71:609–21.
[25] Zel'dovich YaB, Raizer YuP. Physics of shock waves and high-temperature hydrodynamic phenomena. New York: Academic Press, 1966.
[26] Fisher VI, Maron Y. Unpublished.
[27] Lee RW, Nash JK, Ralchenko Y. JQSRT 1997;58:737–42.
[28] Ralchenko, et al. JQSRT;to appear.